

---

## Polarimetric and Photometric Studies of Lunar Samples

A. Dollfus and J. E. Geake

*Phil. Trans. R. Soc. Lond. A* 1977 **285**, 397-402

doi: 10.1098/rsta.1977.0080

---

### Email alerting service

Receive free email alerts when new articles cite this article - sign up in the box at the top right-hand corner of the article or click [here](#)

## Polarimetric and photometric studies of lunar samples

BY A. DOLLFUS

*Observatoire de Paris, Meudon, France*

AND J. E. GEAKE

*U.M.I.S.T., Manchester*

The polarization of scattered light has been investigated for lunar samples from six Apollo and two Luna missions. Over a wide range of the phase angle between incidence and observation directions, the light is found to be polarized only either normal (called positive) or parallel (negative) with respect to the incidence/observation plane. The resulting characteristic curves, of degree of polarization versus phase angle, are indicative of surface properties: the maximum value of polarization is inversely proportional to albedo, for dust-covered surfaces, and the slope is inversely proportional to albedo for most surfaces; the width and depth of the negative-going part of the curve indicate the type and complexity of the surface texture, as confirmed by Stereoscan photographs. This information may now be applied to the determination of albedos and surface textures for objects such as asteroids and planetary satellites, for which no samples are available but for which some polarization measurements have been made.

## 1. INTRODUCTION

The polarization of moonlight has been investigated at Meudon (see Dollfus & Bowell 1970; Geake *et al.* 1970; Dollfus 1971; Dollfus *et al.* 1971*a, b*, 1975; Bowell *et al.* 1972, 1973), ever since the classic work of Lyot (1929); it proved to be a powerful technique for the remote identification of the lunar surface texture long before direct exploration was achieved. The acquisition of lunar samples made it possible to investigate the process in much more detail, as the polarization characteristics of different types of lunar material could be related to their surface textures as observed with a scanning electron microscope. Relationships have now been found between polarization parameters and surface properties, such as albedo and texture. In effect, the lunar samples have been used to elucidate and calibrate the polarization technique, which can now be used to investigate the surfaces of other solar-system objects, such as asteroids and planetary satellites, for which samples are unlikely to be obtained, but for which at least some polarization measurements are possible.

## 2. POLARIZATION PARAMETERS

When unpolarized light is scattered by a rough surface it tends to become partially plane polarized. The degree of polarization  $P$  is found to depend on the phase angle  $V$  – the angle between the incident ray and the direction of observation; the plane of polarization is found to be only either normal to the incidence/observation plane (called, by convention, positive) or parallel to it (called negative). A graph of  $P$  (in parts/10<sup>3</sup>) against  $V$  (deg) gives a polarization curve characteristic of the surface, and figure 1*a* shows some typical results for a sample of lunar fines, at each of five wavelengths. The important features of the curves are

measured by the parameters defined in figure 1*b*:  $P$  reaches a maximum value  $P_{\max}$ , which is wavelength-dependent and usually occurs for  $V$  between  $95$  and  $120^\circ$ . The curve also has a negative-going part, of width  $V_0$  and depth  $P_{\min}$ , which is almost independent of wavelength: figure 1*c* shows this, on a larger scale, for the lunar fines sample. Another useful parameter is the initial slope  $h$  of the positive-going part (in parts  $10^{-3} \text{ deg}^{-1}$ ) – ideally taken as the average slope over about  $20^\circ$  beyond  $V_0$ .

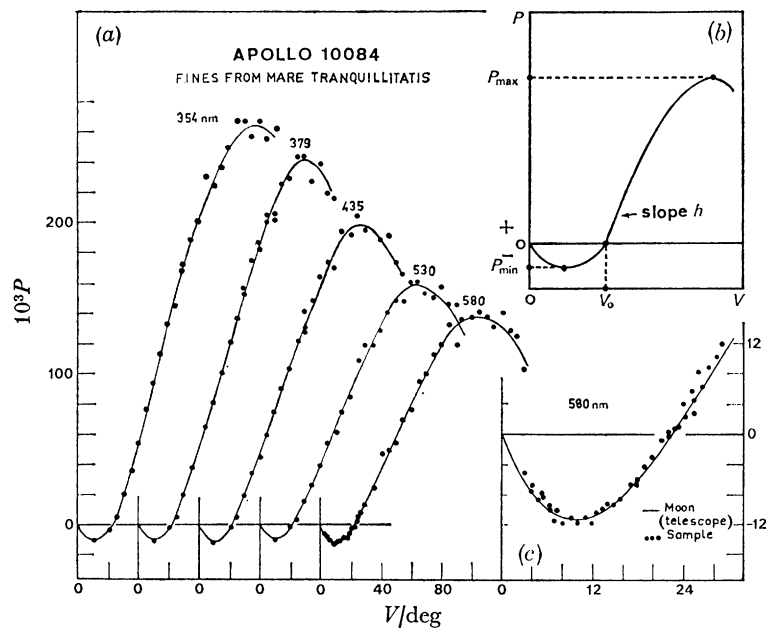


FIGURE 1. (a) Polarization curves (proportional polarization  $P$  plotted against phase angle  $V$ ) for the lunar fines sample 10084.6, at 5 different wavelengths; the scale of  $V$  restarts for each wavelength, in order to separate the curves for clarity. (b) parameters used in analysis; (c) the negative-going part of the 580 nm curve in (a), enlarged, illustrating the agreement between measurements of the lunar sample and of the place on the Moon that it came from; this shows that radiation and erosion have not significantly affected the polarization properties of the lunar surface. (After Geake *et al.* 1970.)

The Moon and lunar dust samples are distinguished by having a polarization curve with a particularly deep negative part, and it was this unusual feature which permitted rather specific identification of the lunar surface texture, as first achieved by Lyot (1929).

### 3. $P_{\max}$ AND $h$ , AND THEIR RELATION TO ALBEDO

Polarization curves have now been obtained for a wide enough range of lunar samples to enable some relation between polarization parameters and surface properties to be established; for example, it has been found that for lunar fines samples  $P_{\max}$  is inversely proportional to the albedo  $A$  (Dollfus *et al.* 1971*a*). This is demonstrated in figure 2, where  $P_{\max}$  is plotted against  $A$  (on a log-log scale) and the relation is found to be linear within the accuracy permitted by the scatter of the points. Earlier telescopic observations of the Moon were found to lie in a narrow strip below this line and parallel to it; however, it was concluded that this displacement was caused by systematic errors in the albedo measurements of the Moon itself, which were then corrected by making use of the relation established by laboratory measurements of lunar fines. Terrestrial rock powders, which have less complicated surfaces than the fairy-castle structures

characteristic of lunar fines, also tend to lie on a straight line, but it is a different one that lies above the line for lunar fines, as shown dotted in figure 2. Lunar rock samples, as shown by circles in figure 2, do not appear to follow any law, but are scattered in the region above the lines. No points are found in the area below the line representing lunar fines, which is evidently a forbidden region.

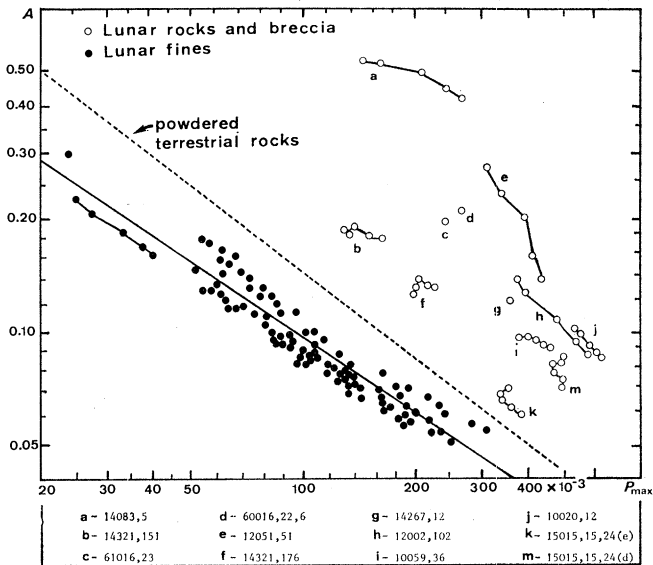


FIGURE 2

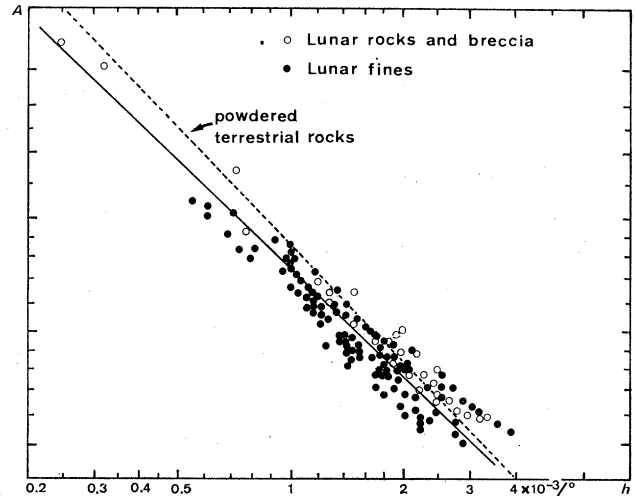


FIGURE 3

FIGURE 2. Maximum value of polarization  $P_{\max}$  plotted against albedo  $A$ , for lunar fines, rocks and breccia; the linked points are for the same sample at different wavelengths. A similar plot for powdered terrestrial rocks is represented by the dotted line.

FIGURE 3. Slope  $h$  of the polarization curve (averaged over the first  $20^\circ$  after  $V_0$ ) plotted against albedo  $A$ , for lunar fines, rocks and breccia; samples and symbols as for figure 2.

A straight-line relation is also obtained when the initial slope  $h$  of the positive-going part of the polarization curve is plotted against albedo, as shown in figure 3 which represents the same samples as figure 2. However, this relation has the property that, unlike the previous one, it is relatively insensitive to the type of surface, and all materials lie close to the same line.

There is in fact a slight tendency for lunar rocks and powdered terrestrial rocks to lie near the line shown dotted in figure 3, and for lunar fines to differ from all the other samples in following a slightly lower line, as shown: however, this small difference represents the only effect of the full range of surface textures, from the complicated fairy-castle structure of the fines to the simpler terrestrial powders and dust-free lunar rocks. This relation was originally discovered by Widorn in 1967 and has been investigated in detail by Zellner (see *Bowell et al.* 1973) and by Veverka & Noland (1973). As the slope/albedo relation is almost independent of surface texture, it is therefore useful in determining the albedos of objects whose surface type is not known. It is also an advantage that less of the polarization curve is required in order to obtain the albedo from the slope than is needed to find it from  $P_{\max}$ , thus enabling albedos to be determined for many more planetary bodies, such as asteroids, which can only be observed from Earth over a limited range of phase angle. Furthermore, from the albedo, the apparent magnitude, and the known distance, the mean diameter can be determined for objects too small to resolve telescopically (*Zellner et al.* 1974).

If a planetary surface is known to be dust-covered, and if  $P_{\max}$  is obtainable, then the  $P_{\max}/$  albedo relationship provides the more accurate way of determining its albedo, because the slope/albedo relation is less precisely established. Furthermore, if the whole polarization curve is available, and if the albedos obtained by the two methods are in agreement, this provides some confirmation that the surface is in fact dust-covered. However, information about the surface texture is more readily obtained from the negative part of the polarization curve.

#### 4. THE NEGATIVE PART OF THE POLARIZATION CURVE AND ITS RELATION TO SURFACE TEXTURE

The dominant characteristic of the polarization curve for the Moon itself, and for the lunar fines samples, is a deep negative-going part at small phase angles, as shown in figure 1*c*. This feature is found to be associated with surfaces consisting of fine opaque grains arranged in a complex way: the 'fairy-castle' structures observed for lunar fines under a microscope show an extreme example of the type of surface required. This strong negative polarization appears to be associated with multiple scattering and shadowing effects, and some progress in explaining it theoretically in these terms has been made by Hopfield (1966) and Wolff (1975). Lunar rock chips, even when they have some adhering dust, have a less complex surface and their polarization curves show a smaller negative-going part; for dust-free rock chips it is smaller still. It is found that the width ( $V_0$ ) and the depth ( $P_{\min}$ ) of the negative part are the

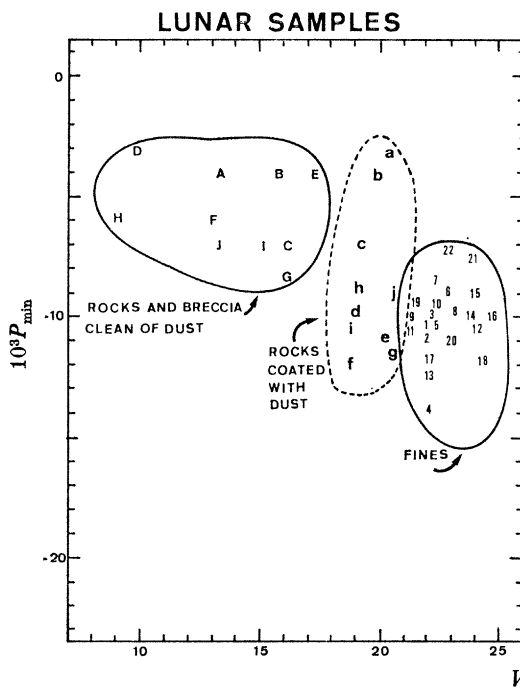


FIGURE 4

FIGURE 4. Width  $V_0$  plotted against depth  $P_{\min}$  for the negative part of the polarization curve for lunar samples. Fines (numbers), dust-coated rocks (lower-case letters), and dust-free rocks (capital letters) are seen to occupy three different regions.

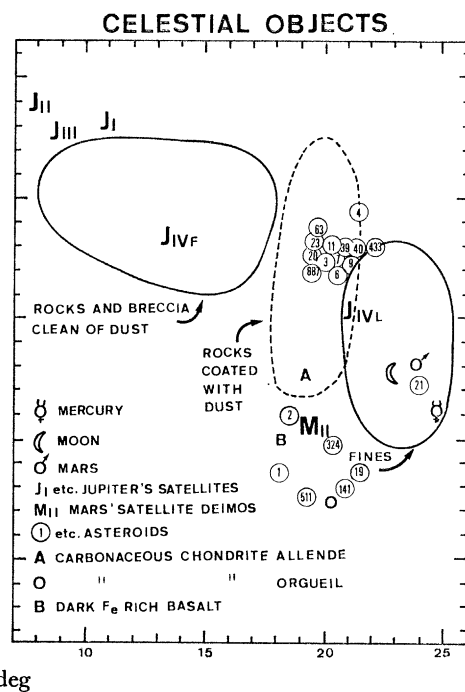


FIGURE 5

FIGURE 5. As figure 4, for atmosphereless solar-system objects; the boundaries of the three regions in figure 4 are superimposed.

two parameters most indicative of surface texture, as demonstrated in figure 4 where their values are plotted for a wide variety of lunar samples. It can be seen that the lunar fines samples occupy a compact region corresponding to a deep and wide negative part, while the dust-free rock chips are in a quite different region, representing a narrower and shallower negative part. Rock chips that were found by stereoscan inspection to be partially dust-covered come in between, and overlap the fines region in extreme cases. This information can now be used to identify the surface types of other planetary bodies (Dollfus 1971), and figure 5 illustrates this application:  $V_0$  and  $P_{\min}$  are plotted for all the atmosphereless objects in the Solar System for which this information is available, and the regions representing the three types of surface in figure 4 are superimposed upon it. These results are discussed fully elsewhere (Dollfus & Geake 1975), and will only be summarized here.

The Moon is represented in figure 5 by an average for the whole disk, and this point comes within the region representing lunar fines, confirming that the relevant microtexture of the samples has not been significantly affected by the sampling and handling processes. Furthermore, telescopic polarization measurements have been made on local areas of the Moon down to a diameter of 10"; these are not shown here, but they all fall within the fines region, suggesting that none of these areas contain significant proportions of exposed rock. Mars also lies in the fines region, and Mercury is near it, indicating that they too are regolith-covered as they are massive enough to retain impact debris; however, as Mars has an atmosphere, the complexity of microtexture represented by its position on the diagram must be of some form other than the lunar-type fairy-castle structure which is characteristic of high-vacuum conditions.

The asteroids are mostly too small to retain a regolith: only Lutitia (21) resembles lunar fines; the rest appear to be rock, thinly covered with dust. They are shown to fall very clearly into two groups, which are also found to have different albedos. The lower and darker group is in the same region as the powdered carbonaceous meteorite samples, and the Mars satellite Deimos also falls within it. Three of Jupiter's satellites show little negative polarization and are also of high albedo, which may indicate a frosty surface; however, Callisto ( $J_{IV}$ ) appears to be dust-covered on its leading hemisphere in its orbital motion ( $J_{IV,l}$ ), and dust-free on its following hemisphere ( $J_{IV,f}$ ).

Finally, all the information in this paper may be combined by representing it in a three-dimensional plot of  $A$ ,  $P_{\min}$ , and  $V_0$ ; this presentation will be discussed in a later paper.

This review is based on many telescopic and laboratory polarization measurements, including those made by C. Titulaer, E. Bowell and B. Zellner. We are grateful to T. Lebertre, J. P. Perrault and M. Duseaux for assistance with the analysis, to Prof. A. Cailleux for geological advice, and to the Textile Technology Department, U.M.I.S.T., for Stereoscan facilities. We are grateful for financial support from C.N.R.S. (Meudon) and S.R.C. (U.M.I.S.T.), and to N.A.S.A. and the U.S.S.R. Academy of Sciences for the loan of the lunar samples.

## REFERENCES (Dollfus &amp; Geake)

- Bowell, E., Dollfus, A. & Geake, J. E. 1972 *Proc. 3rd Lunar Sci. Conf., Geochim. cosmochim. Acta Suppl.* **3**, **3**, 3103–3126.
- Bowell, E., Dollfus, A., Zellner, B. & Geake, J. E. 1973 *Proc. 4th Lunar Sci. Conf., Geochim. cosmochim. Acta Suppl.* **4**, **3**, 3167–3174.
- Dollfus, A. & Bowell, E. 1970 *Astron. & Astrophys.* **10**, 29–53.
- Dollfus, A., Bowell, E. & Titulaer, C. 1971a *Astron. & Astrophys.* **10**, 450–466.
- Dollfus, A. 1971 *Proc. IAU Conf. Physical studies of minor planets.* (ed. T. Gehrels), NASA SP-267, Washington.
- Dollfus, A. & Geake, J. E. 1975 *Proc. 6th Lunar Sci. Conf., Geochim. cosmochim. Acta Suppl.* **6**, **3**, 2749–2768.
- Dollfus, A., Geake, J. E. & Titulaer, C. 1971b *Proc. 2nd Lunar Sci. Conf., Geochim. cosmochim. Acta Suppl.* **2**, **3**, 2285–2300.
- Geake, J. E., Dollfus, A., Garlick, G. F. J., Lamb, W., Walker, G., Steigmann, G. A. & Titulaer, C. 1970 *Proc. Apollo 11 Lunar Sci. Conf., Geochim. cosmochim. Acta Suppl.* **1**, **3**, 2127–2147.
- Hopfield, J. J. 1966 *Science, N.Y.* **151**, 1380–1381.
- Lyot, B. 1929 Thesis, University of Paris: English translation 1964, NASA TT F-187, Washington.
- Veverka, J. & Noland, M. 1973 *Icarus* **19**, 230–239.
- Wolff, M. 1975 *Appl. Opt.* **14**, 1395–1405.
- Zellner, B., Gehrels, T. & Gradie, J. 1974 *Astron. J.* **79**, 1100–1110.